Experimental verification of the Interpolation Method on a real damaged bridge

2015 J. Phys.: Conf. Ser. 628 012045

(http://iopscience.iop.org/1742-6596/628/1/012045)

Journal of Physics: Conference Series **628** (2015) 012045 doi:10.1088/1742-6596/628/1/012045

Experimental verification of the Interpolation Method on a real damaged bridge

M P Limongelli [1], **A Morassi**[2]
[1]Politecnico di Milano, Department of Architecture, Built Environment and Construction Engineering, Milano, Italy.
[2]Università degli Studi di Udine, Department of Civil Engineering and Architecture, Udine, Italy.

E-mail: mariagiuseppina.limongelli@polimi.it

Abstract. The identification of damage in a bridge from changes in its vibrational behavior is an inverse problem of important practical value. Significant advances have been obtained on this topic in the last two-three decades, both from the theoretical and applied point of view. One of the main problems when dealing with the assessment of vibration based damage identification methods is the lack of experimental data recorded on real damaged structures. Due to this, a large number of damage identification algorithms are tested using data simulated by numerical models. The availability of data recorded on a damaged bridge before its demolition gave the authors the uncommon chance to verify the sensitivity and reliability of the IDDM basing on data recorded on a real structure. Specifically data recorded on a reinforced concrete single-span supported bridge in the Municipality of Dogna (Friuli, Italy) were used to apply the damage localization algorithm. Harmonically forced tests were conducted after imposing artificial, increasing levels of localized damage. In this paper the sensitivity of the method is discussed with respect to the number of instrumented locations and to the severity of the damage scenarios considered

1. Introduction

The interest in evaluating the structural health condition basing on non-destructive vibrational methods has significantly increased over the past few decades. Changes in the dynamic characteristics of the structure can indicate the emergence of possible damage occurring during the structure lifetime and provide quantitative estimates of the level of residual safety. Among vibration-based damage-detection methods [1], [2], those based on changes in modal shapes or their derivatives, and on frequency response functions (FRFs), are particularly effective allowing the localization of damage in addition to its detection, when variations of the deformed shape of the structure are taken into account in the definition of the damage feature. One of the main problems when dealing with the assessment of vibration based damage identification methods is the lack of experimental data recorded on real damaged structures. Due to this, a large number of algorithms have been tested using data simulated by numerical models that in many cases are affected by simplifications and assumptions that somehow alter the correct representation of reality. For example the effect of nonlinearities, soil-structure interaction, non-structural components but also experimental errors or environmental and operational changes, is often neglected when working on numerical models. On the contrary full scale testing such as for example those reported at references [3]-[5] allows taking into account all the phenomena contributing to the real behaviour of the structure thus providing an effective mean to check the performances of methods and algorithms for damage identification.

The availability of data recorded on a damaged bridge before its demolition gave the authors the uncommon chance to verify, using data recorded on a real structure, the sensitivity and reliability of the

[1] corresponding author

recently proposed Interpolation Damage Detection Method. Specifically, data recorded on a reinforced concrete single-span supported bridge in the Municipality of Dogna (Friuli, Italy), were used to apply the damage localization algorithm. The bridge consists of a slab supported by three longitudinal beams simply supported at the ends. Harmonically forced tests were conducted after imposing artificial, increasing levels of localized damage. In this paper the sensitivity of the IDDM is discussed with respect to the number of instrumented locations and to the frequency range considered for the estimation of the damage index. A couple a variants in the definition of the damage index are investigated as well with reference to the experimental data recorded on the bridge.

2. The basis of the IDDM for damage localization

The method applied herein to identify the location of damage is the Interpolation Damage Detection Method previously presented [6], [7] for the case of seismically excited structures. The damage detecting feature in the IDDM is defined in terms of the error related to the use of spline functions in approximating the *displacement profile* of the bridge. Specifically, the modeling accuracy at a given location of the bridge is defined as the difference between the displacement profile actually measured and the displacement profile computed at that same location by interpolating the measured displacements at all the other locations. The possible increase of the interpolation error at one instrumented location between a reference (undamaged) state and the inspection state (possibly, a damaged state) is assumed to be a symptom of the existence of damage close to the location where the change is detected. The displacement profile, either in the reference and in the inspection phase, is defined in terms of the frequency response functions (FRF) of the acceleration. Namely, for each frequency value, the values of the transfer functions between the acceleration at the measurement points and the input acceleration provide the "*Operational Deformed Shape*" (ODS) at that frequency. At the *l*-th location z_l and at the frequency f_i, the spline interpolation error is defined as the difference of the transfer function $H_R(z_l,f_i)$ calculated from the recorded signals, and the function $H_S(z_l,f_i)$ calculated through interpolation of the transfer functions $H_R(z_k,f_i)$ at all the other instrumented locations, with $k \neq l$, that is

$$H_S(z_l, f_i) = \sum_{j=0}^{3} c_{j,l}(f_i)(z_l - z_{l-1})^j \,, \tag{1}$$

where the coefficients (c_{0l}, c_{1l} c_{2l} c_{3l}) are functions of the values $H_R(z_k, f_i)$ at locations $\{z_k\}_{k=1}^{n}$, e.g., $c_{j,l}(f_i) = g(H_R(z_k, f_i))$, $k \neq l$. In terms of FRFs the interpolation error at location *z (*in the following the index *l* will be dropped for clarity of notation) at the *i*-th frequency value f_i, is defined as the difference between the magnitudes of recorded and interpolated FRFs:

$$E(z, f_i) = \left| H_R(z, f_i) - H_S(z, f_i) \right|, \tag{2}$$

where H_R is the FRF of the response recorded at location *z* and H_S is the spline interpolation of the FRF at *z*. In order to characterize each location *z* with a scalar-valued error parameter, the norm of the error on the whole range of frequencies has been considered:

$$E(z) = \sqrt{\sum_{i=n_o}^{n_o+N} E(z, f_i)^2} \,, \tag{3}$$

where *N* is the number of frequency lines correspondent to the frequency range starting at line n_o, where the signal to noise ratio is high enough to allow a correct definition of the FRF.

The difference between the two values, respectively E_0 and E_d of *E* calculated at location *z* respectively in the baseline (undamaged) and in the inspection (potentially damaged) phases, provides an indication about the existence of a degradation at the considered location:

$$\Delta E(z) = E_d(z) - E_0(z) \,. \tag{4}$$

An increase in the interpolation error, i.e. $\Delta E(z) > 0$, highlights a localized variation in the operational deformed shape and it is assumed to be a symptom of a local variation of stiffness at *z* associated with the occurrence of damage. In order to remove the effect of random variations of $\Delta E(z)$

a threshold is calculated in terms of the mean $\mu_{\Delta E}$ and variance $\sigma_{\Delta E}$ of $\Delta E(z)$ on the population of available values (that is calculated at all the instrumented locations).

$$\Delta E(z) > \mu_{\Delta E} + \nu\sigma_{\Delta E} . \quad (5)$$

The threshold is assumed as a minimum value beyond which a damage is considered to exist at locations where the damage index exceeds the threshold. In our simulations ν takes the values 1 or 2 that, assuming a Normal distribution of this parameter, correspond to accept respectively the 15% and the 2% probability of having a false alarm (threshold exceeded by chance).

Therefore, the damage index $D(z_l)$ at a given location z_l is defined by the relation

$$D(z_l) = \Delta E(z_l) - (\mu_{\Delta E} + \nu\sigma_{\Delta E}), \quad l=1,...,n, \quad (6)$$

Positive values of $D(z_l)$ are assumed to indicate a possible damage occurred at z_l. It should be recalled that if the right hand side of equation (6) is negative, then the damage index is assumed to be equal to zero.

3. A case study: the Dogna Bridge

Dogna Bridge is the four-span, one-lane concrete bridge shown in Figure 1. The length of each span is 16.0 m and the lane is about 4 m width. The bridge deck is formed by a reinforced concrete (RC) slab of 0.18 m thickness, supported by three longitudinal RC beams of rectangular cross-section 0.35×1.20 m. Beams are simply supported at their ends and are connected at the supports, at mid-span and at span-quarters by transverse RC diaphragms. Dynamic tests were performed from April 2 to April 11, 2008 on the end span highlighted in **Figure 2** before the demolition of the bridge. This span was made independent of the adjacent span by removing the deck-joint in correspondence of the pier. Moreover, the asphalt overlay of about 0.1 m thickness was also removed before testing.

Figure 1. General view of Dogna Bridge (left) and detail of damages D1-D6 (right).

We refer to the reference [8] for a complete report on the experiment. Dynamic tests were performed on the bridge in its actual condition (undamaged configuration, indicated by U in what follows) and in seven damaged configurations (D1-D7), see Figure 2. The first six damage states were obtained by cutting a lateral RC beam. The seventh level of damage was obtained by removing the concrete near the mid-span cross-section of the same beam. The vertical motions of the deck structure were produced by means of a vibration generator . The experimental layout is shown in Figure 3. Based on this experimental setup, deck's inertance of the bridge was measured by means of zoom analyses within narrow neighborhoods of natural frequencies. Frequency resolution ranged from 0.02 for the lower modes (up to 15 Hz) to 0.04 Hz for higher modes. The above procedure has been applied for the characterization of all the damaged configurations D1-D7. Figure 4 reports the magnitudes of the FRFs in the undamaged and in three damaged configurations at locations A10 (downstream beam), A11 (central beam) and A14 (upstream beam) considering a linear interpolation for the frequency ranges not measured during the forced vibration tests.

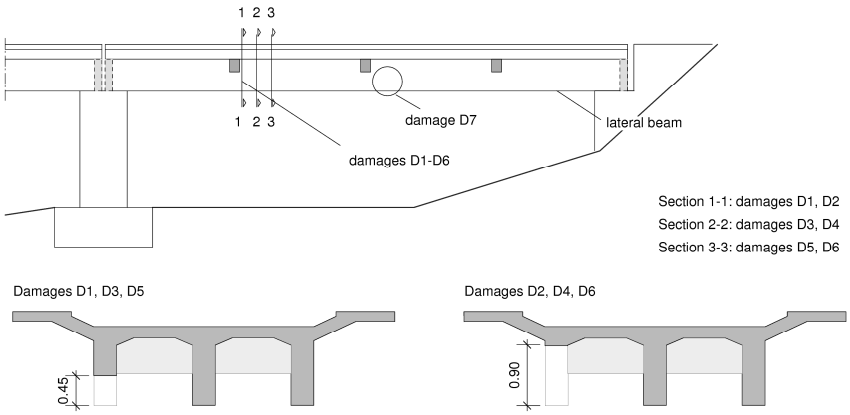

Figure 2. Damaged configurations.

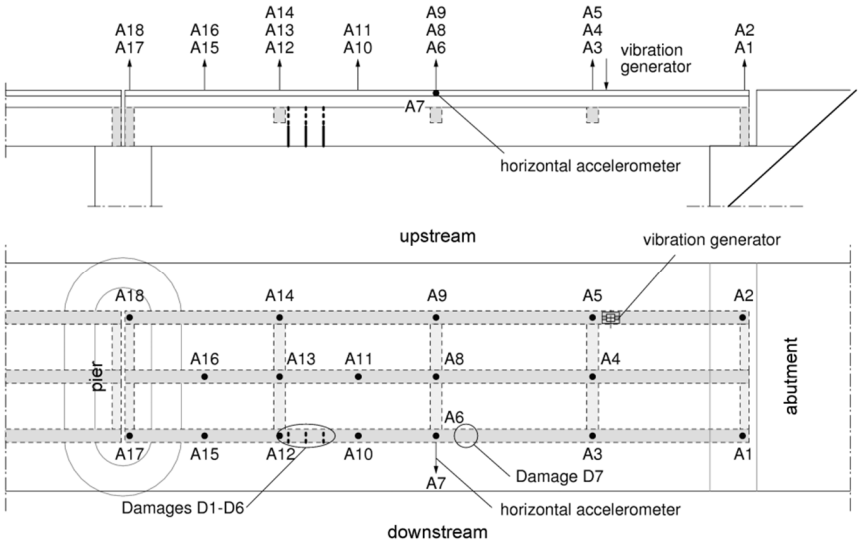

Figure 3. Instrumental layout.

The variations of the first two natural frequencies (around 9 Hz and 13 Hz) are evident from the FRFs at locations A10 and A14 (Figure 4a-c); the evolution of the frequency of the fourth mode (around 35 Hz) can be easily recovered from the FRF associated to location A14 (Figure 4c). The FRFs at location A11 (Figure 4b) are particularly useful to follow the evolution of the frequency of the fifth mode (about 47 Hz). From the undamaged configuration D0 up to configuration D3 a gradual reduction of the frequencies of all the modes 1 to 5 occurs. Starting from configuration D4 and up to D5 the frequencies of all the modes slightly increase. Finally a reduction of all the modal frequencies is exhibited for configurations D6 and D7. This behavior has already been pointed out in previous papers. Particularly, we refer to reference [9] for an interpretation of the dynamic tests and for structural identification analysis on Dogna Bridge. All the measured vibration modes have dominant vertical components.

4. Detecting damage on Dogna Bridge

As recalled in Section 3, the bridge was harmonically excited by means of a shaker located at one fourth of the upstream beam. The main aim of the testing was to carry out a modal characterization of the structure; hence responses were measured only within narrow neighborhoods of the expected natural frequencies values and the measured frequency range was adjusted at each test in order to match the current values of natural frequencies. The FRFs at instrumented locations are thus available only in narrow frequency ranges that change from one test to the other. The application of the IDDM requires

through equation (3) and (6), requires that the FRFs are measured in the same frequency range in the reference and in the damaged configurations. In order to calculate the values of the FRF in the frequency ranges where they were not available, a linear interpolation of the measured values was carried out in the range 8-50 Hz. Even if this is a rather crude estimation of the actual values of the FRFs, it allows to correctly detecting the damaged locations, as will be shown in the following.

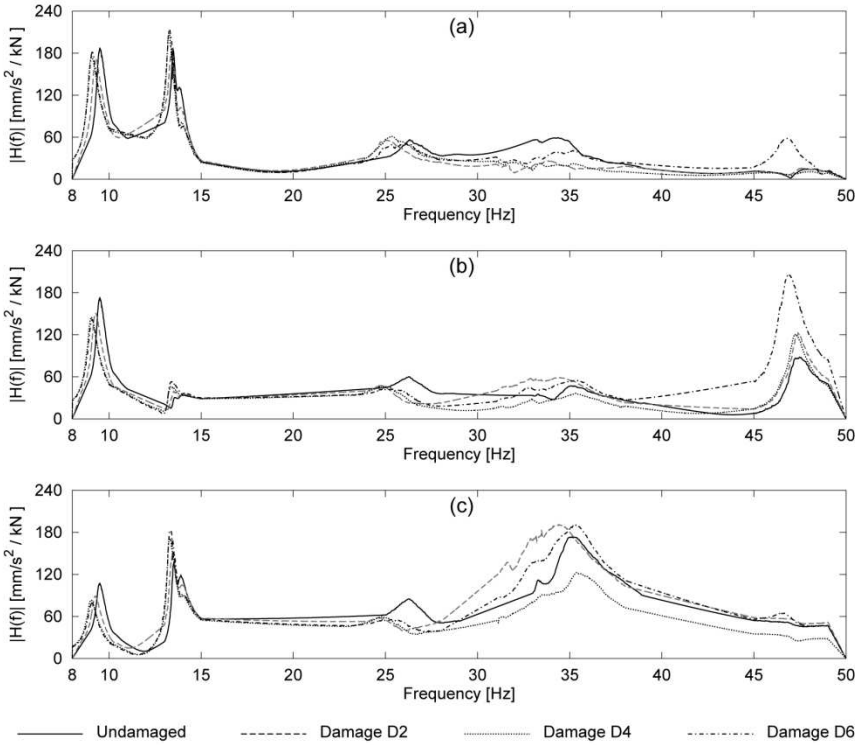

Figure 4. FRF at locations A10 (a), A11 (b) and A14 (c) for configurations U, D2, D4, D6 in the frequency range 8-50 Hz.

In order to investigate the sensitivity of the diagnostic method to the parameters on which the damage feature depends (number of instrumented locations, frequency range for the evaluation of the interpolation error, accepted probability of missing alarm) several analysis where carried out considering different values of these parameters. Referring to the paper [9] for more details, the main findings of the analysis are as follows:

- *Selection of the accepted probability of false alarm P_f through the parameter ν*: Simulations show that the choice ν=2 ($P_f \cong 2\%$) allows for a correct localization of severe damage only and, in addition, the probability of missing alarms turns out to be very high. Conversely, the choice ν=1 ($P_f \cong 35\%$) leads to a better compromise between the probability of having false and missing alarms, compare Figure 5with Figure 6.
- *Number of instrumented locations*: the IDDM was initially applied considering separately the three alignments of sensors at downstream, central axis and upstream. More precisely, the damage index at an instrumented point was evaluated by considering only the FRFs measured at sensors belonging to the same alignment, and neglecting the responses recorded at all the other instrumented locations. Results are reported in Figure 5 and Figure 6 respectively for the two considered values (ν=1 and ν=2) of the probability of false alarm.

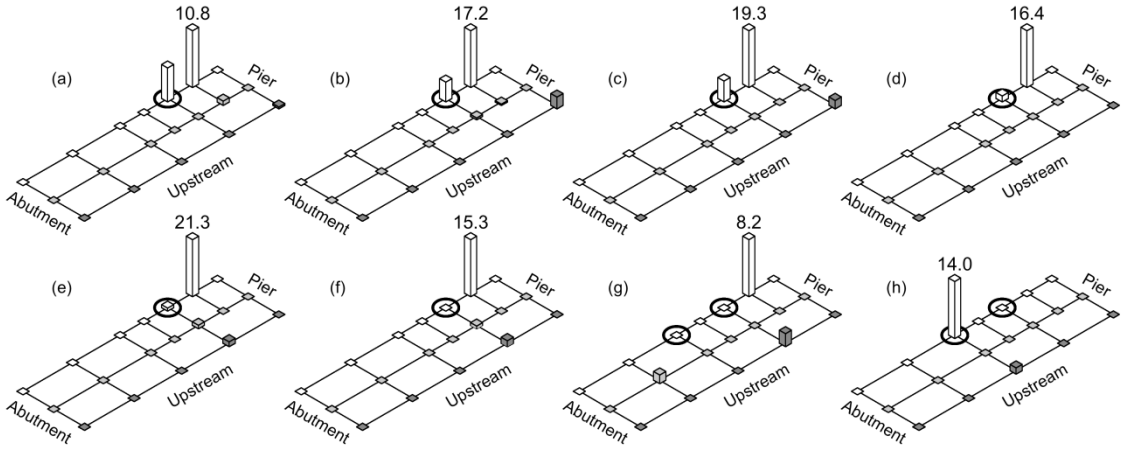

Figure 5. Influence of the probability of the accepted probability of false alarm. **Threshold ν=1**. Damage index D evaluated in the interval 8-38 Hz (first four vibrating modes) from the reference configuration (U) to actual damage configuration: (a) D1; (b) D2; (c) D3; (d) D4; (e) D5; (f) D6; (g) D7; (h) from D6 to D7. Circles denote the actual damage locations.

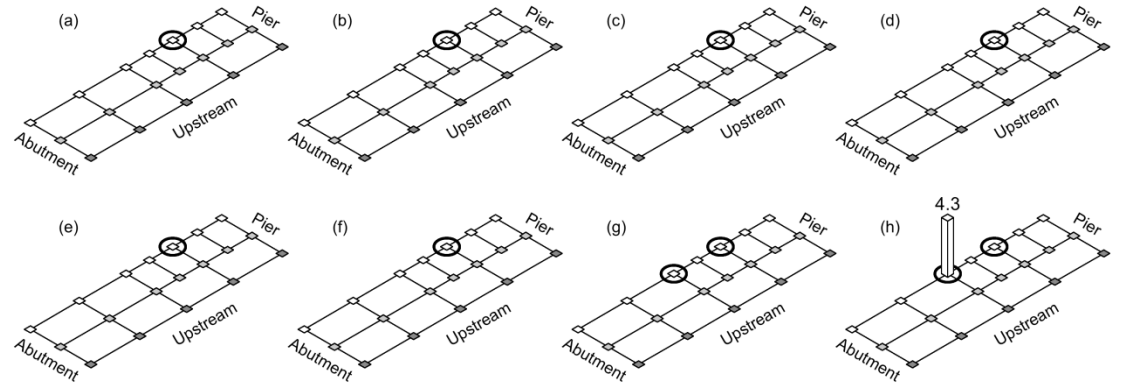

Figure 6. Influence of the probability of the accepted probability of false alarm. **Threshold ν=2.** Damage index D evaluated in the interval 8-38 Hz (first four vibrating modes) from the reference configuration (U) to actual damage configuration: (a) D1; (b) D2; (c) D3; (d) D4; (e) D5; (f) D6; (g) D7; (h) from D6 to D7.Circles denote the actual damage locations.

The above analyses were repeated by including all the instrumented points in the evaluation of the damage index. In Figure 7 and Figure 8 results obtained considering all the instrumented locations for the estimation of the damage feature are reported.

In general terms, the larger amount of data improves the identification and damage localization turns out to be more reliable, whatever the value chosen for the probability of false alarm P_f (ν=1 or ν=2). In particular, false alarms located far from the actual damage position are reduced in number and the performance of the choice ν=2 is now comparable to that resulting from taking ν=1 that is results (reported in Figure 7 and Figure 8) appear less sensitive to the assumption about the accepted probability of false alarm.

A couple of variants in the estimation of the damage parameter $E(z_l, f_i)$ were also investigated. A first variant consists in neglecting the phase information by assuming that the interpolation error $E(z_l, f_i)$ is given as the absolute value of the difference between the modulus of the recorded and interpolated FRFs, namely

$$E(z_l, f_i) = \left\| H_R(z_l, f_i) \right| - \left| H_S(z_l, f_i) \right\| \quad (7)$$

where z_l is the location considered and f_i the ith frequency value. In spite of the reduction in input information, the quality of the identification is comparable to that obtained previously. The identification improves when all the instrumented points are considered and the parameter ν is larger, see, for example, Figure 8 reporting results obtained under the assumption ν=2.

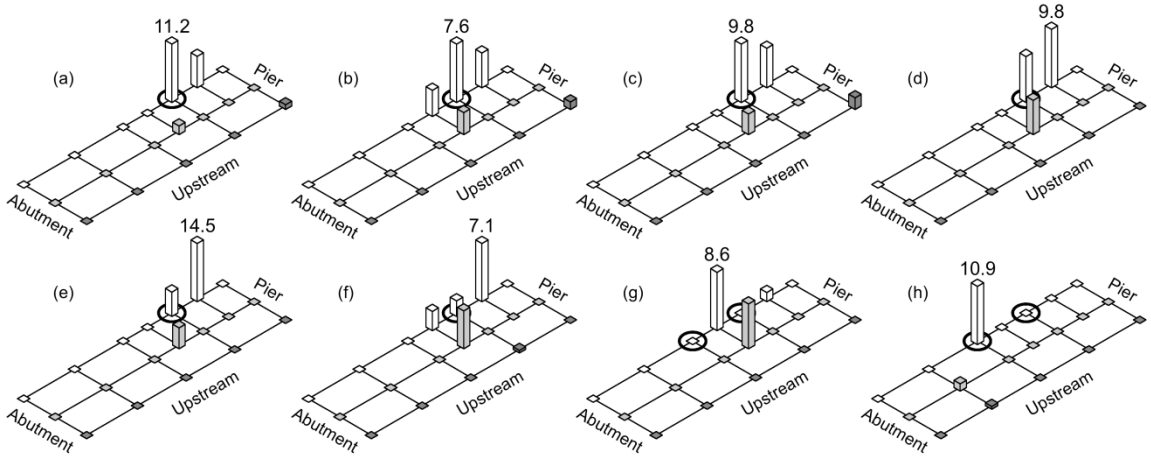

Figure 7. Damage index D evaluated according to equation (8) in the interval 8-38 Hz (first four vibrating modes) from the reference configuration (U) to actual damage configuration: (a) D1; (b) D2; (c) D3; (d) D4; (e) D5; (f) D6; (g) D7; (h) from D6 to D7. **Threshold ν=1** and all the instrumented points are considered in the evaluation of the damage index.. Circles denote the actual damage locations.

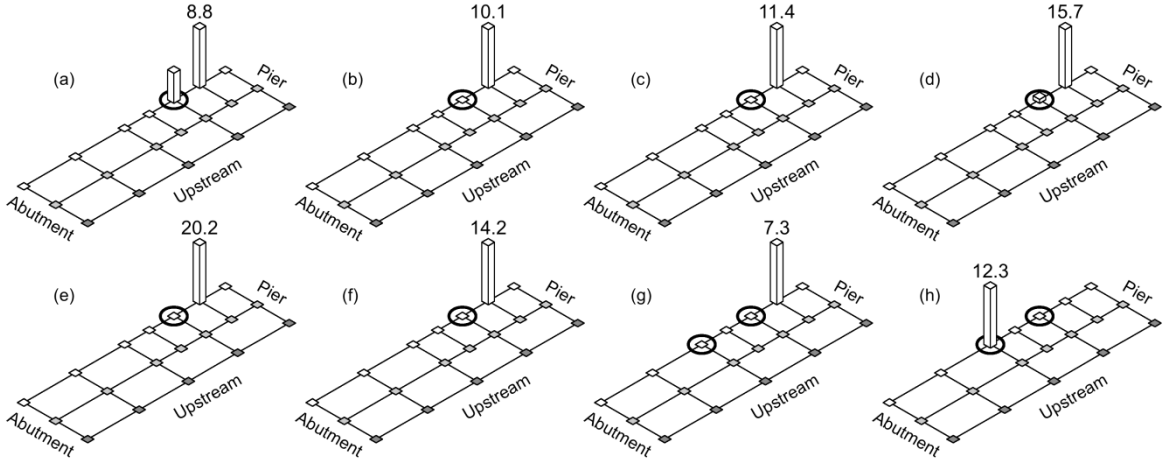

Figure 8. Damage index D evaluated according to equation (8) in the interval 8-38 Hz (first four vibrating modes) from the reference configuration (U) to actual damage configuration: (a) D1; (b) D2; (c) D3; (d) D4; (e) D5; (f) D6; (g) D7; (h) from D6 to D7. **Threshold ν=2** and all the instrumented points are considered in the evaluation of the damage index. Circles denote the actual damage locations

In a second variant, the sensitivity of the IDDM to different extension of experimental FRFs outside the measuring ranges was investigated. In particular, the values of the FRFs were reconstructed in the whole range 0-50 Hz was basing on their analytical expression and using the values of the modal parameters of the first five modes recovered from the Experimental Modal Analysis of the bridge.

Despite the high accuracy of the local reconstruction of experimental FRFs, see reference [10], significant discontinuities in the magnitude of the FRFs occur at frequencies corresponding to the boundary between measured and reconstructed FRFs. Overall, the quality of the damage localization worsens with respect to using a linear interpolation to estimate the FRFs. This can be attributed to discontinuities in the reconstructed FRFs due to the extension of the local approximation of the FRFs from the narrow neighborhoods of the natural frequencies to the whole range 0-50 Hz. Furthermore, as previously recalled, the measurement frequency ranges (hence their boundaries) changed from one test to the following leading to a shift of the discontinuities in the frequency domain that makes the comparison of the FRF corresponding to different damaged configurations quite unreliable.

5. Conclusions

In the paper the sensitivity of the Interpolation Damage Detection Method to several parameters is investigated using experimental data recorded on the Dogna bridge, a four-span, one-lane, reinforced concrete real damaged structure. The influence of both experimental conditions (number of instrumented locations, frequency range of the measurements) and of managing decisions (value of the accepted probability of false alarm) were studied with reference to data relevant to the several damaged scenarios inflicted to the bridge.

Results show that the accuracy of the damage localization increases with the amount of the available experimental data, both in terms of instrumented locations and in terms of frequency range of the measured responses. Furthermore, the increase in the amount of available experimental make results less sensitive to the choice of the accepted probability of false alarm.

6. Acknowledgments

The present work was partially supported by the ReLuis-DPC Executive Project 2014-2016, Special Project “Monitoring”, whose contribution is gratefully acknowledged.

7. References

[1] Fan W, Qiao P 2008. Vibration-based damage identification methods: a review and comparative study. *Structural Health Monitoring*; 10(1) p.83–29.
[2] Yan Y J, Cheng L, Wu Z Y, Yam L H 2007 Development in vibration-based structural damage detection technique. *Mechanical Systems and Signal Processing*; 21(5) p.2198–2211.
[3] Cruz P J S , Salgado R 2008 Performance of vibration-based damage detection methods in bridges. *Comput-Aided Civ. Inf.* 24 p. 62–79.
[4] Teughels A, De Roeck G 2004 Structural damage identification of the highway bridge Z24 by FE model updating. *J. Sound Vibr.* 278 p. 589–610.
[5] Toksoy T, Aktan A E 1994 Bridge-condition assessment by modal flexibility. *Exp. Mech.* 34(3) p. 271–278.
[6] Limongelli M P 2010 Frequency response function interpolation for damage detection under changing environment. *Mech. Syst. Signal Pr.* 24(8) p. 2898–2913.
[7] Limongelli M P 2011 The interpolation damage detection method for frames under seismic excitation. *J. Sound Vibr.* 330 p. 5474–5489.
[8] Dilena M, Morassi A 2011 Dynamic testing of a damaged bridge. *Mech. Syst. Signal Pr.* 25(5) p. 1485–1507.
[9] Dilena M, Limongelli M P, Morassi A 2015 Damage localization in bridges via FRF interpolation method, *Mech. Syst. Signal Pr.* 52-53 p. 162-180.
[10] Dilena M, Morassi A, Perin M 2011 Dynamic identification of a reinforced concrete damaged bridge. *Mech. Syst. Signal Pr.* 25(8) p. 2990–3009.